Optimization of the experimental parameters of the ligase cycling reaction

Niels Schlichting[1], Felix Reinhardt[2], Sven Jager[2], Michael Schmidt[2], and Johannes Kabisch[1,*]

[1]Department of Biology, Computer-Aided Synthetic Biology, TU Darmstadt, Darmstadt, Germany and
[2]Department of Physics, Computational Biology and Simulation, TU Darmstadt, Darmstadt, Germany

*Corresponding author: E-mail: johannes@kabisch-lab.de

Abstract

The ligase cycling reaction (LCR) is a scarless and efficient method to assemble plasmids from fragments of DNA. This assembly method is based on the hybridization of DNA fragments with complementary oligonucleotides, so-called bridging oligos (BOs), and an experimental procedure of thermal denaturation, annealing and ligation. In this study, we explore the effect of molecular crosstalk of BOs and various experimental parameters on the LCR by utilizing a fluorescence-based screening system. The results indicate an impact of the melting temperatures of BOs on the overall success of the LCR assembly. Secondary structure inhibitors, such as dimethyl sulfoxide and betaine, are shown to negatively impact the number of correctly assembled plasmids. Adjustments of the annealing, ligation and BO-melting temperature further improved the LCR. The optimized LCR was confirmed by validation experiments. Based on these findings, a step-by-step protocol is offered within this study to ensure a routine for high efficient LCR assemblies.

Key words: ligase cycling reaction, DNA assembly, secondary structures, computer-aided bridging oligo design

Introduction

One of the aims of synthetic biology is to specify, design, build and test genetic circuits, and this goal requires rapid prototyping approaches to facilitate assembly and testing of a wide variety of circuits. To this end, many assembly methods were used in the last decades to build DNA constructs, e.g., Gibson assembly (1), Golden Gate assembly (2, 3), circular polymerase extension cloning (4), biopart assembly standard for idempotent cloning (5) and yeast homologous recombination (6). Some of these methods require specific modifications of the DNA parts such as overhangs or restriction sites, which hamper the reusability, while other methods leave scars. Additionally, DNA part standardization approaches, e.g., the BioBrick-system, result in sequence redundancies which have a negative impact on assembly efficiencies (7).

In contrast, the ligase cycling reaction (LCR) fulfills the prerequisites for automated assemblies and uses phosphorylated DNA parts (8–11). The assembly order is determined by single-stranded oligonucleotides building a bridge [so-called bridging oligonucleotides (BOs)] between adjacent parts. BOs are typically designed based on general rules provided by the literature (9, 10). One important parameter for the LCR assembly is the melting temperature (T_m) of the BOs at around 70°C for each half to facilitate optimal hybridization of template and oligonucleotide for given cycling parameters. Closely related is the free energy ΔG, which is assumed as the more important quantity for oligonucleotide-based biological experiments (12, 13). In the LCR, its impact is counteracted by using dimethyl sulfoxide (DMSO) and betaine to increase ΔG and thus to reduce secondary structures (9, 10). Nevertheless, the roles of ΔG-related crosstalk and the potential of ΔG-optimized BOs in the LCR have not been investigated so far.

The literature offers several tools regarding LCR optimization. Nowak *et al.* (14) provide a tool for the assembly of DNA that codes for a protein, where they return both the DNA fragments as well as the BOs to minimize unwanted effects. The tool considers codon mutations, as long as they encode the same amino acid, and is intended to be applied for LCR-based gene synthesis. Bode *et al.* (15) offers similar functionality. Another web-application includes the design of primers and performs T_m and ΔG cross-checks for the oligonucleotide sequences against themselves, their DNA probes and whole genomes (13) but is not applied for the LCR. Robinson *et al.* (16) use a BO-design-tool with an adjustable target melting temperature but without optimizing the crosstalk. An experimental perspective is given by de Kok *et al.* (9), where a design-of-experiment approach and multivariate data analysis were used to assess the impact of a wide range of parameters including the concentrations of the secondary structure inhibitors DMSO and betaine. The following study starts with these baseline conditions. The LCR is investigated with the scope on the impact of the choice of BOs, their intramolecular and intermolecular crosstalk and the context of the experimental temperatures. For this, a toy-model plasmid and fluorescence-based readout is utilized (graphical abstract: Figure 1) to detect and validate the influence of all parameters and to generate new rules for an optimized LCR assembly. Finally, the new LCR conditions are used to assemble two additional plasmids to verify the findings.

Materials and methods

Toy-model plasmid for the optimization experiments

All LCRs for the optimizations were performed with a toy-model plasmid made of seven fragments (Figure 1B), with a total length of 4918 bp. This plasmid consists of six inserts and the plasmid cloning vector CloneJet pJET1.2/blunt (2974 bp; Thermo Fisher Scientific, MA, USA). For the inserts, two genes of fluorescent proteins, *sfGFP*, *mRFP1*, were ordered at Addgene (www.addgene.org: pYTK001, pYTK090; 17) and split into three subparts each to increase size heterogeneity, so that the plasmid fragment length ranges from 79 bp to 2974 bp. Additionally, the same terminator BBa_B0015 was used in both fluorescent protein genes to further increase assembly complexity. A spacer sequence 'S' of 37 bp was added to prevent the ligation of part 3 with part 7 (Figure 1B). For all *in silico* cloning, the software Geneious was utilized (v. 11.0.5, http://www.geneious.com, 18). A GenBank-file of the toy-model plasmid is available in the supplement and at www.gitlab.com/kabischlab.de/lcr-publication-synthetic-biology.

Part amplification

Primers for the amplification (Eurofins Genomics, Ebersberg, Germany) were phosphorylated by the T4-polynucleotidekinase/-buffer (New England Biolabs, Ipswich, USA) prior to amplification *via* polymerase chain reaction (PCR; Q5® High-Fidelity
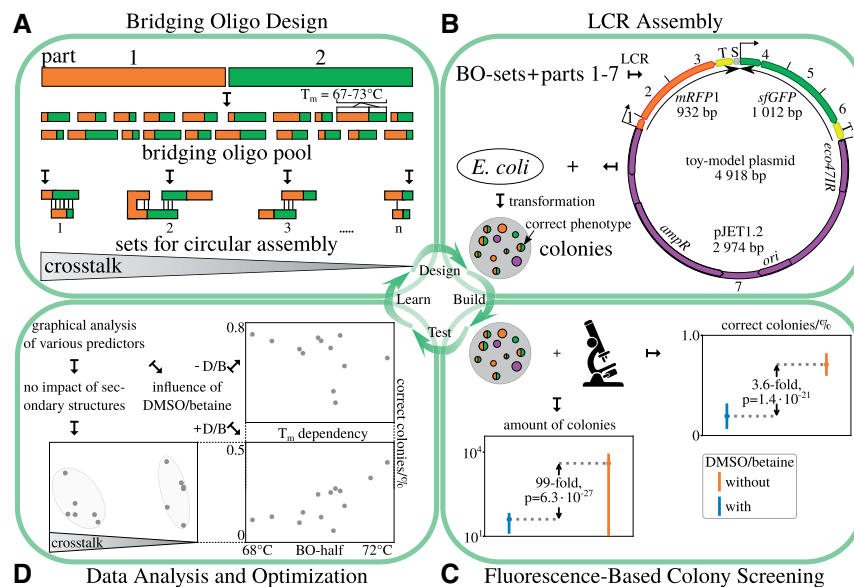

Fig. 1 Workflow for the LCR optimization. (**A**) Bridging oligo-sets (BO-sets) were designed using general design rules with the focus on ΔG-related BO-crosstalk while maintaining a T_m of $70 \pm 3°$C. (**B**) In total, 25 sets were designed, including one manually designed set using the software Primer3, and utilized for the LCR assembly of a toy-model plasmid. The plasmid consists of seven parts with lengths in the range of 79 bp to 2974 bp and a total length of 4918 bp. It contains two genes for fluorescent proteins, *mRFP1* and *sfGFP*, and a vector. Both fluorescent protein genes were split into three subparts (*mRFP1*: parts 1–3, *sfGFP*: parts 4–6). The same terminator BBa_B0015 (T) was used twice to simulate sequence redundancies. A DNA-spacer S (37 bp) was added at the end of part 3 to avoid hybridization of the BO utilized for the ligation of parts 6 and 7. The sequences of all parts are shown in Supplementary Table S1. (**C**) The toy-model plasmid enables a fast and reliable fluorescence-based readout to observe the LCR efficiency and the total amount of colonies to investigate various LCR conditions. Based on this method, a significant negative impact by using the baseline LCR conditions (8% v/v DMSO, 0.45 M betaine) was revealed for the seven-part toy-plasmid. The P-values were derived from a Kolmogorov–Smirnov test between the two sets of data shown in Supplementary Figures S4 and S5. (**D**) With the focus on all BO-sets, no ΔG-related impact was detected in the baseline and DMSO/betaine-free LCR conditions. Further graphical analysis of the BO-sets revealed an association of the average BO-T_m, the efficiency and total amount of colonies. Finally, the optimizations were applied on another split of the toy-plasmid (three-part design: 1. *mRFP1*, 2. *sfGFP*, 3. vector) and two validation plasmids (Supplementary Figures S18 and S19). *ampR*, gene for ampicillin resistance; $\pm D/B$, with or without DMSO and betaine; *eco47IR*, gene for a restriction enzyme (reduction of religations of the vector); *mRFP1*, monomeric red fluorescent protein 1; *ori*, origin of replication; *sfGFP*, superfolder green fluorescent protein; T_m, melting temperature.

Polymerase, New England Biolabs, Ipswich, USA). Forward and reverse primers were phosphorylated separately in 50 μl total volume with 4 μM primer, 4 mM adenosine triphosphate and 10 U of T4-polynucleotidekinase for 1 h at 37°C and 20 min at 65°C for the denaturation. The low primer concentration was chosen because it is beneficial for the enzymatic phosphorylation. The 79 bp promoter of *mRFP1* (part 1, Figure 1B) was ordered as forward and reverse strand (lyophilized, salt-free). Both strands were phosphorylated separately as described for the amplification primers, followed by an annealing procedure to obtain double-stranded DNA (3 min at 95°C and 70 cycles of 20 s with an incremental decrease of 1°C). The backbone-part pJET1.2/blunt was PCR-amplified using a template containing a lacZ coding sequence (pJET1.2/blunt-*lacZ*). Choosing primers which omit *lacZ* during PCR allows to screen for plasmid-carryover through blue-white screening. The *lacZ* does not exist in the final sequence of the toy-model plasmid. Afterwards, all PCR products were DpnI-digested (60 min at 37°C; inactivation: 20 min at 80°C), purified (column-based NEB Monarch® PCR & DNA Cleanup Kit; New England Biolabs, Ipswich, USA) and the DNA quantity/quality was measured by photometry (Spectrophotometer UV5Nano, Mettler Toledo, Columbus, USA). Afterwards, the phosphorylated primers and DNA parts were stored at −20°C. The sequences of the amplification primers are shown in Supplementary Table S2. The sequences of the toy-model parts are shown in Supplementary Table S1.

BO design

BOs were predicted according to the rules given in de Kok *et al.* (9): they were all orientated in forward direction and designed at specific concentrations of 10 mM Mg^{2+}, 50 mM Na^+, 3 nM plasmid parts, 30 nM BOs and 0 mM dNTPs. Geneious asks for a concentration of dNTPs but they are not utilized in the LCR. Though, the concentration has to be adjusted to 0 mM. All BOs were ordered lyophilized from Eurofins Genomics (Ebersberg, Germany) as salt-free custom DNA oligonucleotides. Quality was checked by Eurofins Genomics *via* matrix-assisted laser desorption ionization-time of flight or capillary electrophoresis.

One BO-set was designed manually with the melting temperature tool of Primer3 (19), which is distributed with the software suite Geneious. For the T_m calculation and salt correction, the nearest-neighbor algorithm and the corresponding salt correction by SantaLucia (20) were utilized to design a BO-set with melting temperatures of 70°C for each half-BO. Primer3 only accepts a single DNA concentration, despite the experiment using different concentrations of parts and BOs. As prompted by Geneious, only the BO concentration of 30 nM was inputted. This manual set is denoted by an 'M'.

To investigate the crosstalk of BOs, additional sets were designed by minimizing or maximizing ΔG-dependent crosstalk between oligonucleotides while maintaining a T_m between 67°C and 73°C. Crosstalk is based on secondary structure and among others defined as the sum of all minimum free energies (MFEs) when cofolding each oligonucleotide of a BO-set with each oligonucleotide in that set and with itself. As a reference temperature for the crosstalk calculations, the annealing temperature of the multi-step LCR protocol was used (55°C, 9). As with the manual set, the SantaLucia parameters were utilized for the T_m calculations. Additionally, the DNA part concentration was adjusted to 3 nM to match the experiment. The impact of DMSO and betaine were not considered for the calculations of the MFEs. Sets with minimized crosstalk are denoted by 'L' for low crosstalk and sets with maximized crosstalk by a 'H' for high crosstalk. All BO-sets, sequences and melting temperatures are provided in Supplementary Table S3 and are available at www.gitlab.com/kabischlab.de/lcr-publication-synthetic-biology. Further details on the BO design are given in the Supplementary data (21–27).

Ligase cycling reaction

For the assembly, the purified PCR products were mixed with supplements with the following concentrations: 1×-Ampligase® ligase buffer, 0.5 mM NAD+, 3 nM of toy-plasmid parts 1–6, 0.45 M betaine and 8% v/v DMSO. In contrast to de Kok *et al.* (9), the concentration of the vector pJET1.2/blunt (part 7) was reduced to 0.3 nM to achieve fewer religations of the vector. Positive effects of increasing the molar insert-to-vector ratio were already described for other cloning methods (28, 29) and were confirmed in preliminary LCRs (data not shown). LCRs using these experimental concentrations, i.e., the manually designed BOs and the cycling conditions described in the next paragraph, are referred to as baseline conditions. A 10×-Ampligase® reaction buffer was self-made with the concentrations described by the manufacturer of the Ampligase® (Lucigen, WI, USA). NAD+ was supplied separately by using a self-prepared 10 mM stock solution. BO-sets were premixed in nuclease-free water with 1.5 μM of each BO, heated up for 10 min at 70°C and cooled down on ice before adding them to the split master-mixes. Subsequently 7.5 U of Ampligase® (Lucigen, WI, USA) was added. After mixing by inverting and centrifugation, each LCR was split typically in three ($n = 3$) reactions with a cycling-volume of 3 μl. LCR-quintuplets ($n = 5$) were used to investigate the impacts of crosstalk and utilizing or omitting DMSO/betaine, which are presented in Figure 2 and Supplementary Figures 5 and 12. After the cycling, all LCRs were cooled down on ice to recondense evaporated liquid in the PCR-tubes, and centrifuged.

For the cycling, a DNA Engine Tetrad® 2 thermal cycler, 96-well Alpha™ Unit cycling block and low-profile PCR stripes (Bio-Rad Laboratories GmbH, Muenchen, Germany) were utilized. The speed of ramping used for all LCRs was 3°C s⁻¹. The cycling was initiated by a denaturation step at 94°C for 2 min, followed by 25 cycles at 94°C for 10 s, 55°C for 30 s and 66°C for 1 min. In contrast to the published protocols (9, 10), 25 cycles instead of 50 cycles were used due to the low total LCR volume of 3 μl. Afterwards, either 30 μl electrocompetent or chemically competent NEB® 10-β *Escherichia coli* cells (New England Biolabs, Ipswich, USA) were transformed as described in the following paragraph.

Electroporations were performed serially for each single LCR. For this, each LCR condition was transformed in a non-batch-wise manner to reduce workflow-derived influences, so that, e.g., each condition was transformed once before proceeding with the second replicates. (i) Cells were mixed from a master-aliquot for each experiment with one LCR-replicate of one LCR condition, (ii) suspension was transferred to a cuvette, (iii) an electric pulse was applied (2.5 kV), (iv) 450 μl SOC-medium were added, (v) the cell-suspension was transferred to a tube, (vi) the tube was put for 1 h in a thermal cycler for recovery and (vii) finally the suspension was plated on agar plates. After the recovery, an appropriate volume of the transformation mix was plated on Lysogeny Broth (Miller) plates containing 1% m/v agar and 100 μg ml⁻¹ ampicillin to get a total amount in the range of 10–200 colony forming unit (CFUs) per plate. The plates were grown for 15 h at 37°C.
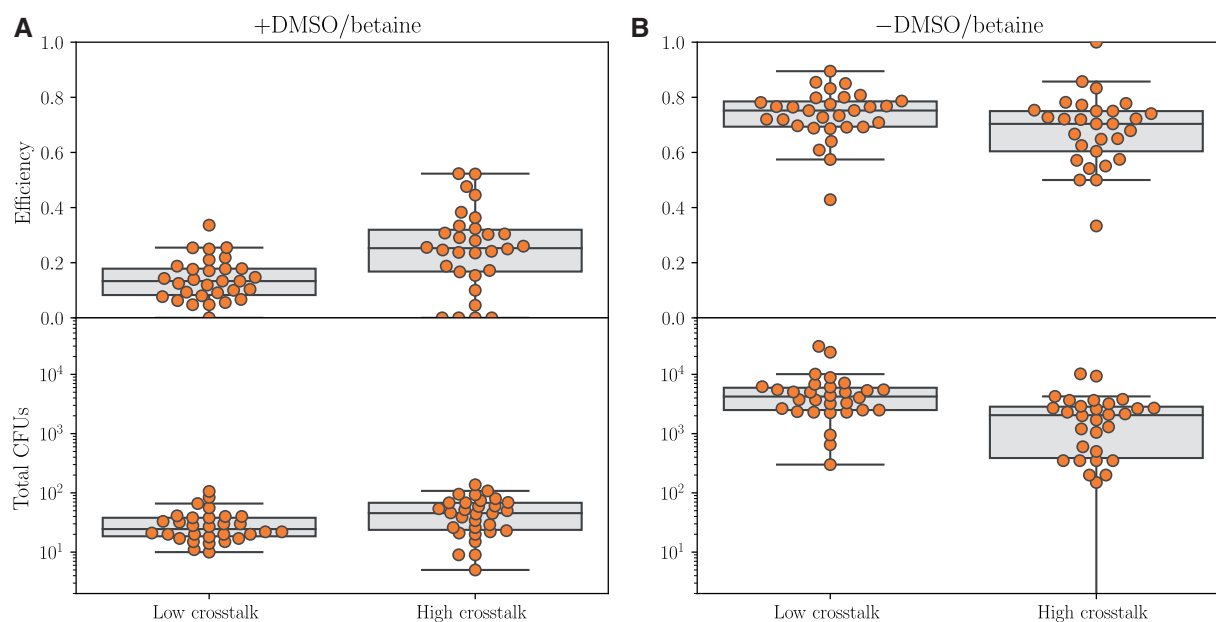
Fig. 2 Overview of the seven-part LCR of the toy-model plasmid by utilizing six bridging oligo-sets (BO-sets) with low crosstalk and six BO-sets with high crosstalk. Each BO-set was used five times to assemble the toy-model plasmid (Figure 1B) by using the baseline conditions with 8% v/v DMSO/0.45 M betaine and without both detergents. For all LCRs, 3 μl were transformed by electroporation in 30 μl NEB® 10-β E. coli cells. For more detailed results of each BO-set refer to Supplementary Figures S4 and S5. (**A**) The baseline conditions with DMSO and betaine resulted in low efficiencies and low amounts of colonies. No correlation between crosstalk and BO performance was found. (**B**) LCRs without DMSO and betaine resulted in more colonies and higher efficiencies in comparison to the baseline conditions. The sequences of all BO-sets are shown in Supplementary Table S3. BO, bridging oligo; CFU, colony forming unit; DMSO, dimethyl sulfoxide.

For chemical transformations, the experiments were performed in a parallel manner: (i) cells were mixed from a master-aliquot for each experiment with all replicates of all LCRs in a 96-well PCR-plate using a multi-channel pipette, (ii) the suspensions were incubated on ice for 30 min, (iii) the heat-shock of 30 s was applied in a PCR-cycler by using 96-well PCR-plates, (iv) the suspensions were placed on ice for 10 min and (v) 170 μl SOC-medium were added to all LCR-cell-mixes followed by recovery of 1 h and plating as described for the electroporations.

Colony screening and plasmid sequencing

By transforming the LCRs into E. coli, the toy-model plasmid enables a fluorescence-based discrimination of correct (red- and green-fluorescent CFUs) and misligated plasmids (red or green or non-fluorescent CFUs). To investigate the LCR assembly, the efficiencies of all LCRs were determined by observing the phenotype of ampicillin-resistant CFUs via fluorescence microscopy (microscope: Axio Vert.A1, Carl Zeiss Microscopy GmbH, Jena, Germany, 50×-magnification; LEDs for sfGFP/mRFP1: 470/540–580 nm). To calculate the LCR efficiency, the phenotypes of all CFUs per LCR were screened. For plates with more than 100 CFUs, 100 colonies were screened randomly by first picking the spot of interest macroscopically followed by the observation with the microscope. The efficiency was obtained by dividing the number of correct CFUs by the total number of microscopically observed CFUs. The phenotypes of the CFUs were determined by visual observation only. An example image of all phenotypes is shown in Supplementary Figure 3.

The amount of CFUs per 3 μl was obtained from the total CFUs per plate and the used plating volume and dilution.

To validate this fluorescence-based system, plasmids from 120 CFUs with different phenotypes were isolated with the Monarch® Plasmid Miniprep Kit (New England Biolabs,

Ipswich, USA) and analyzed via Sanger-sequencing (Eurofins Genomics, Ebersberg, Germany) to correlate them with the genotypes.

Graphical analysis

Unless specified otherwise, T_m calculations in the following sections were performed with the thermodynamic parameters and salt correction by SantaLucia (20) and the divalent salt conversion by von Ahsen et al. (30). The shown T_ms are of half-BOs. Each half-BO is complementary to the DNA part that it is designed to attach to. A BO is the direct concatenation of two half-BOs. Dangling ends and coaxial stacking were not included in the calculation. Error bars are the standard deviation with Bessel's correction. The average T_m of a BO-set is obtained from all half-BOs of the set.

Validation experiments

For the validation experiments two additional plasmids-constructs were split in three and seven parts (Supplementary Figures S18 and S19) and were assembled using the baseline and two optimized conditions (Table 1) derived by the results of the toy-model plasmid. Both plasmids and splits are similar in size range in comparison to the toy-model plasmid with *sfGFP* and *mRFP1*. GenBank-files of the validation plasmids are available in the supplement and at www.gitlab.com/kabischlab.de/lcr-publication-synthetic-biology. In the validation plasmids the *lacZ* and two or one antibiotic resistance genes were split into subparts (Supplementary Figures S18 and S19). This enables a blue-white screening of correct assembled plasmids (blue colonies) and misassembled ones (white) by plating them on agar with the antibiotics and X-Gal/isopropyl β-D-1-thiogalactopyranoside (IPTG). For both plasmids, 3 μl per LCR were transformed in 30 μl NEB® 10-β E. coli cells.

Table 1 Summary of the LCRs for the validation experiments using the toy-model plasmid and the validation plasmids 1 and 2 (Figure 1B, Supplementary Figure S18 and S19)

Factor	Unit	LCR protocol			Protocol	Toy-model plasmid (TP)		Validation plasmid 1 (VP1)		Validation plasmid 2 (VP2)	
		Baseline	75°C	Improved		3 parts	7 parts	3 parts	7 parts	3 parts	7 parts
DMSO	% v/v	8	8			Efficiency (%)					
Betaine	M	0.45	0.45		Baseline	37 ± 6	0 ± 0[a]	88 ± 4	17 ± 29[a]	98 ± 2	93 ± 12
Annealing temperature	°C	55.0	55.0	66.0	Improved	47 ± 6	17 ± 7[a]	96 ± 1	98 ± 3[a]	95 ± 0	93 ± 3
Target T_m for each bridging oligo half	°C	70.0	74.8	67.8		Total CFUs (per 3µl LCR)					
					Baseline	250 ± 46	6 ± 3[a]	125 ± 8	1 ± 1[a]	365 ± 63	12 ± 2
					Improved	559 ± 33	30 ± 14[a]	493 ± 19	323 ± 70[a]	2023 ± 331	189 ± 26

Each plasmid was split into three and seven parts which were assembled by using the baseline and improved LCR protocol. The LCRs were transformed in chemically competent cells by a heat-shock.

[a]For results, the LCRs were transformed by electroporation due to low or no colonies when chemical transformation was used.

BO, bridging oligo; CFU, colony forming unit; DMSO, dimethyl sulfoxide; T_m, melting temperature of a BO-half using the calculation of SantaLucia (20).

For the validation plasmid 1, the transformed cells was transferred to lysogeny broth (LB) agar plates with 100 µg ml^{-1} spectinomycin after one hour of recovery followed by an overnight incubation for 16 h at 37°C. Forty CFUs were transferred to agar plates containing spectinomycin, 50 µg ml^{-1} kanamycin, 40 µg ml^{-1} X-Gal and 200 nM IPTG by using sterile tooth picks to identify colonies with correct assembled and misassembled plasmids. After 16 h, all transferred colonies were checked for a blue/white phenotype and empty spots were regarded as kanamycin sensitive. Blue colonies represented correct assembled plasmids. White colonies and empty spots were treated as misassembled plasmids. To calculate the efficiency for each LCR the amount of blue colonies was divided by the amount of transferred CFUs. Ten plasmids of blue, spectinomycin and kanamycin resistant colonies were sequenced *via* Sanger sequencing. Further, four plasmids of white, spectinomycin and kanamycin resistant colonies were analyzed.

For the validation plasmid 2, the transformed cells were transferred to LB agar plates containing 100 µg ml^{-1} spectinomycin, 40 µg ml^{-1} X-Gal and 200 nM IPTG. After the incubation of 16 h at 37°C, all colonies per plate were checked for a blue/white phenotype. For the calculation of each LCR efficiency, the amount of blue colonies were divided by the sum of blue and white colonies. As described for the validation plasmid 1, Sanger sequencing of plasmids from ten colonies with the correct phenotype 'blue' and plasmids from four colonies with the wrong phenotype 'white' was used to validate the results.

Results and discussion

Toy-model plasmid offers robust system to investigate LCR assemblies

To simulate a challenging SynBio-construct for the investigations of the LCR, a toy-model plasmid was designed (Figure 1B). This plasmid consists of seven parts of varying size (79 bp to 2974 bp) and the same BioBrick terminator sequence BBa_B0015 in both fluorescent protein genes. To investigate the LCR different BO-sets, experimental parameters, a toy-model plasmid and fluorescence-based analysis were used. For the analysis and optimization, ~100 CFUs/LCR (if available) were screened *via* visual observation by using fluorescence microscopy to calculate the efficiency of each assembly reaction. The four observable phenotypes 'non-fluorescent', 'green fluorescent', 'red fluorescent' and 'green + red fluorescent' are demonstrated in

Supplementary Figure S3. The amount of CFUs per 3 µl LCR was determined by macroscopic counting of all colonies per agar plate and extrapolation by using the dilution-factor. In total, 61 different experimental conditions were tested and more than 15 000 colonies were screened by fluorescence-microscopy to obtain the assembly efficiencies. In contrast to the vector concentration of 3 nM in the literature (9, 10), the concentration was decreased to 0.3 nM to counteract religations.

No fluorescent CFUs were obtained in the control reactions without the ligase (Supplementary Figure S5). Additionally, blue-white screening of about 1000 non-fluorescent CFUs revealed no carry-over of the template used for the amplification of the vector pJET1.2/blunt. A carry-over of the templates pYTK001 or pYTK090 used for the amplification of *sfGFP* and *mRFP1* was not possible due to a change of the antibiotic resistance marker gene.

To validate the fluorescence-based readout, the observed phenotypes of 120 CFUs with different phenotypes were correlated with the corresponding plasmids *via* Sanger sequencing. The analyzed plasmids from 60 CFUs with a bicolored fluorescence (red and green) contained all seven DNA parts in the correct order/orientation when compared with the *in silico* sequence of the toy-plasmid. Sequencing results of 60 plasmids with a different phenotype (20 plasmids from only green fluorescent CFUs, 20 plasmids from only red fluorescent CFUs and 20 plasmids from non-fluorescent CFUs) indicated that they lacked at least one *sfGFP*-subpart or *mRFP1*-subpart (still red or green) or were religated vector (no fluorescence). The latter phenotype was also observed for plasmids with missing subparts of both fluorescent protein genes in preliminary experiments. Point-mutations in the LCR products were regarded as errors introduced by amplification primers, PCRs or *E. coli* and were not treated as LCR-misassemblies since they occurred outside of the ligation areas.

In our experiments, the misassembled plasmids from green fluorescent colonies lacked at least one subpart of the *mRFP1*. Interestingly, about 10–100 bp of both ends of the missing subparts were still existent. For the 20 analyzed CFUs with only the red fluorescent phenotype, the plasmids lacked the spacer sequence at the 3'-end of the *mRFP1* and the entire *sfGFP*. This suggests that *E. coli* can recognize the 129 bp BBa_B0015 terminator that is used for both *sfGFP* and *mRFP1* and delete it by *recA*-independent recombination (31, 32). Thus repetitive sequences in the LCR assembly cause misassemblies. Related to this, the BO that spans parts 6 and 7 can partly hybridize with the

terminator in part 3 and may negatively influence the ligation. This suggests that duplicates at the end of DNA parts negatively influence LCR efficiency.

Another issue is related to the heterogeneous LCR-mixture, which contains the desired DNA fragments, debris of these fragments from PCRs, amplification primers and PCR templates (even if they are digested and purified). *E. coli* may circularize any linear DNA in the mixture. The subsequent transformation of *E. coli* enables a ring closure by endogenous mechanisms and the growth of CFUs containing the religated vector or plasmids with missing parts. This was observed in the control reaction without ligase in Supplementary Figure S5. Thus the carry-over of DNA in combination with the ability of *E. coli* to ligate linear DNA contributes both to the amount of misassembled plasmids and correct plasmids.

In summary, the fluorescence-based screening of colonies employed here is a valid and fast (manually: ~500 CFUs h^{-1}) method to determine the assembly efficiencies and to investigate the influence of changing parameters in the LCR. A correlation of the phenotype and genotype is a useful tool without the need for next generation sequencing and offers an objective true–false readout by microscopy (as utilized for these studies) or photometric analysis of images (using e.g. OpenCFU, 33; CellProfiler, 34).

Influence of DMSO, betaine and the T_m of BOs on LCR assemblies

Thirteen different BO-sets, with sequences given in Supplementary Table S4, were used to assemble the toy-model plasmid made of seven fragments. Two separate experiments were performed with different conditions. The baseline LCR used 8% v/v DMSO and 0.45 M betaine, whereas the crosstalk-increased LCR did not use any DMSO or betaine (Figure 2).

On average, the LCRs with both detergents revealed 3.6× lower efficiencies and 99× fewer total CFUs per 3 µl in comparison to assemblies without DMSO and betaine (P < 0.001, Figure 1C; raw data in Supplementary Figure S4). Further confirmation of these results can be seen in Supplementary Figures 12 and 14 in more consistent experiments using the same batches of DNA parts and competent cells. Graphical analysis of various predictors revealed no ∆G-related effects for assembling the toy-plasmid for both experimental setups (Figure 2, Supplementary Figure S6A and B; more predictors in Supplementary Figures S7–S10). Guanine or cytosine at the 3′-end of BOs were not found to affect the LCR. Notably, the conditions without DMSO and betaine resulted in less red fluorescent phenotypes for all utilized BO-sets (Supplementary Figure S4). Apparently, this phenotype is mainly related to *recA*-independent deletion by *E. coli*. Probably, the omission of both detergents is beneficial for assemblies with repetitive sequences.

For LCRs with DMSO and betaine, BO-related differences were detected, e.g., the LCR using BO-set L1 was less efficient than using H1 (Supplementary Figure S5A). Further analysis of the used BO-sets revealed an impact of the melting temperature despite the T_ms of all sets being similar ranging from 68°C to 72°C (Supplementary Figure S6C). The set with a BO-T_m of 68°C had an efficiency of 10% whereas the set with a BO-T_m of 72°C showed an efficiency of 50%. This suggests that a melting temperature higher than 72°C may result in even better assemblies for LCRs with DMSO and betaine. This is confirmed by recalculating the melting temperatures of the set of sequences designed to have a T_m of 70°C by de Kok *et al.* (9), who used the SantaLucia parameters with the salt correction by Owczarzy

et al. (35). We have found the average T_m of these half-BOs to be 72.2°C when calculated using these parameters. When using the SantaLucia parameters and SantaLucia salt correction as has been done so far in this study, the T_m is found at 74.8°C. The impact of different salt corrections is illustrated in Supplementary Figure S11. Overall, for LCRs with 8% v/v DMSO and 0.45 M betaine, a BO target temperature above 70°C was found to be beneficial.

Investigation of the Primer3 source code used for the design of the manual BO-set and comparison with SantaLucia (20) revealed that the code expects both concentrations to be identical and to sum up to the input amount. Thus the prompted BO concentration of 30 nM corresponds to part and BO concentrations of 15 nM. Due to this, the manual BO-set had an average T_m of 71.5°C (Supplementary Figure S6) when evaluated in full accordance with the SantaLucia formula instead of the targeted 70°C.

An alternative approach to obtain higher assembly efficiencies without rising costs due to synthesizing longer oligonucleotides is to omit DMSO and betaine. This omission also aids automated liquid handling approaches because both detergents have unfavorable properties like extreme viscosities, hygroscopic characteristics and acting as surfactants. These new experimental conditions greatly improved both the efficiency and total number of CFUs (Supplementary Figure S5). Consistent with the results of the LCRs with DMSO/betaine, the melting temperature is the most influencing parameter. As a result of the omission of DMSO and betaine, BO-sets with lower T_ms became favorable, yielding the greatest total amount of colonies at high efficiency (Supplementary Figure S6D). This behavior is also observed by comparing the total CFUs derived by utilizing the BO-sets L2, H1 and the manual one (Supplementary Figure S12). Similar to this seven-part toy-plasmid, another LCR-design with a T_m-independent BO design (20 bp for each BO-half) was published by Roth *et al.* (11) where six parts in a range of 79–2061 bp were assembled with high efficiencies. The *Taq*-ligase and a two-step LCR protocol with annealing and ligation at the same temperature of 60°C were utilized. This supports our findings that the omission of DMSO and betaine and to increase the annealing temperature can be helpful for ligation-based DNA assemblies.

An explanation for low efficiencies in the baseline LCR is related to the large difference between the annealing temperature of 55°C and ligation temperature of 66°C in combination with the utilization of DMSO and betaine. Both detergents reduce the energies required for strand separations (36, 37). Together with the experimental temperatures, this may result in an extensive reduction of template for the ligase by separating already hybridized BO/probe double strands. BO-sets with lower T_ms are theoretically more affected than sets with higher melting temperatures and should benefit from decreasing the temperature interval. Related to this, a reduction of the ligation temperature is expected to be advantageous. This was validated by using three BO-sets with different melting temperatures (Supplementary Figure S13) despite the ligation temperature of 60°C being lower than the optimum temperature of the ligase (according to the manufacturer: 70°C). Increasing the annealing temperature, which would also decrease the interval, was assumed to be disadvantageous due to accelerated BO/template-separation and was not investigated.

Several mechanisms are suspected to cause the total CFU decrease in LCRs with DMSO/betaine. First, lower LCR efficiencies result in fewer fully assembled plasmids and fewer colonies. The effects of DMSO and betaine were also investigated

separately to prove these results (Supplementary Figure S14). Second, DMSO/betaine negatively influence the electroporation process. This can also be seen in Supplementary Figure S14, where an LCR without DMSO/betaine was mixed with both detergents before the electroporation and 3–4× fewer CFUs were obtained in comparison to DMSO/betaine-free controls. In contrast to the literature (9, 10), a lower volume-ratio of LCR and cells was used for the transformations (1:10; 2× higher concentration of DMSO/betaine). These conditions are not toxic for the *E. coli* strain NEB® 10-β because chemical transformations of the same strain with the plasmid pUC19 revealed no negative effects of utilizing a combination of DMSO and betaine (Supplementary Figure S17). A negative impact of DMSO and a positive impact of betaine was observed. A strain-dependent influence of DMSO in chemical transformations was described in (38) and such an influence is also plausible for betaine and a combination of both reagents. To counteract the CFU-reducing effects of detergents, a 30 min dialysis using *aq. dest.* and a nitrocellulose-membrane after the LCR was found to increase the amount of colonies (data not shown).

The omission of DMSO/betaine was beneficial for the assembly of the seven-part split of the toy-model plasmid. To investigate optimal experimental temperatures for the new conditions without DMSO and betaine, the interaction of the annealing, ligation and BO-melting temperatures need to be considered.

Increased annealing temperature is beneficial for LCRs without DMSO and betaine

To optimize the LCR without DMSO/betaine, several experiments were performed. Supplementary Figure S6D shows that the BO-sets with low T_ms yield the most correct CFUs, which suggests that the BOs may bind too strongly to unwanted sites and be unavailable for ligation. To counteract this, the optimal annealing temperature was determined by performing a gradient-LCR, i.e., LCRs at different cycling conditions. For this, three new BO-sets were composed from the existing pool of BOs used in LCRs shown in Supplementary Figure S5 to obtain sets with average melting temperatures of 67.8°C, 69.9°C and 71.8°C (sequences in Supplementary Table S4). In an annealing temperature range of 56.5°C to 75.6°C, these sets were analyzed by chemically transforming the corresponding LCRs in chemically competent NEB® 10-β *E. coli*. This resulted in roughly 100× lower transformation efficiency in comparison to the electrocompetent cells utilized in previous experiments.

For all sets, the efficiency was similar throughout the entire temperature range (Figure 3A). Consistent with previous results, the total amount of CFUs increased with lower BO-T_ms (comparing the results shown in Supplementary Figure S6H and Figure 3B). Furthermore, all sets have a global CFU maximum in the annealing temperature range of ∼66–71°C. This range contains the ligase optimum of 70°C, which suggests positive effects of prolonging the total ligation time to 1.5 min (30 s annealing at 66–68°C, 1 min ligation at 66°C) in comparison to the baseline condition of 30 s annealing at 55°C and 1 min ligation at 66°C.

In total, increasing the annealing temperature from 55°C to 66°C improved the CFU yield of every BO-set by a factor of two without a loss of efficiency. The BO-set '67.8°C' performed better than the other sets. Supplementary Figure S16 shows that at the optimum annealing temperature of 67.8°C, the BO-set '67.8°C' also showed slightly greater efficiency than the other sets.

Lower BO-melting temperatures may have additional benefits for LCR assemblies without DMSO and betaine. To validate

this, new BO-sets with lower melting temperatures of 62°C to 67.3°C were designed and applied for ligations at 66°C (Figure 3C and D, sequences in Supplementary Table S5). Surprisingly, a drop-off in efficiency and CFUs was observed for BO-sets with equal or lower melting temperatures than 66°C. In comparison to the results shown in Figure 3A the efficiency of the 69.9°C-set is 30% lower. This result is most likely related to a loss of function by additional freeze-thaw cycles or contamination of the DNA parts, BO-sets and/or supplements. Negative impacts of repeated freeze-thaw cycles on the DNA parts and BOs were already mentioned for the LCR (16) and for single-stranded oligonucleotides (39). Nevertheless, the total amount of CFUs was further optimized by using BOs with a T_m of 67.8°C for each half and by increasing the annealing temperature in the range of the ligase optimum without decreasing the efficiency. Together with previous optimizations by performing the LCR without DMSO and betaine the assembly of the seven-part was highly improved. For the following experiments, we defined an improved LCR protocol (Table 1).

New LCR protocol improves the assembly of two different toy-model plasmid splits

In order validate the positive effects of omitting DMSO/betaine and to use a higher annealing temperature of 66°C in DMSO/betaine-free conditions, the sequence of the seven-part plasmid was used for a three-part split consisting of *mRFP1* as part 1, *sfGFP* as part 2 and pJET1.2/blunt as part 3. The BOs for this assembly were newly ordered and new aliquots of all LCR supplements were utilized. This plasmid was assembled by using the baseline and improved LCR conditions (Table 1). For the baseline condition, the LCR was performed using the manual BO-set with a T_m of 71.4°C for each half, 8% v/v DMSO, 0.45 M betaine and the annealing at 55°C. For the improved LCR condition, the BO-set had a T_m of 67.8°C for each half (set was already used for the gradient-LCR in Figure 3), no DMSO/betaine were used and the annealing was at 66°C. The sequences of both BO-sets are shown in Supplementary Table S10. In general, the three-part plasmid was built by the two different LCR protocols with no differences in the total plasmid size (4918 bp), sequence and BOs in comparison to the seven-part version. Further, the seven-part split was also assembled by using both protocols.

For both splits of the toy-model, the omission of DMSO and betaine was beneficial (plasmid 'TP' in Figure 4 and Table 1) although the differences are lower in comparison to the optimization experiments. The low efficiencies of the seven-part split without DMSO/betaine in comparison to the high efficiencies obtained in the LCRs shown in Figure 2 are likely related to the repeated freeze-thaw cycles of the DNA parts. Further, the three-part LCR split was transformed in chemically and electrocompetent cells (Supplementary Figure S20). The results indicate that the LCR efficiencies are independent of the transformation method. Interestingly, the amount of colonies are similar for the chemical transformation and electroporation although the pUC19-transformation efficiency of the electrocompetent cells was ∼100× higher. We assume that the negative effects of DMSO/betaine in the electroporation and the higher transformation efficiency (Supplementary Figure S14) compensate each other. For the LCRs without DMSO and betaine, the amount of CFUs was higher when the electroporation was used.
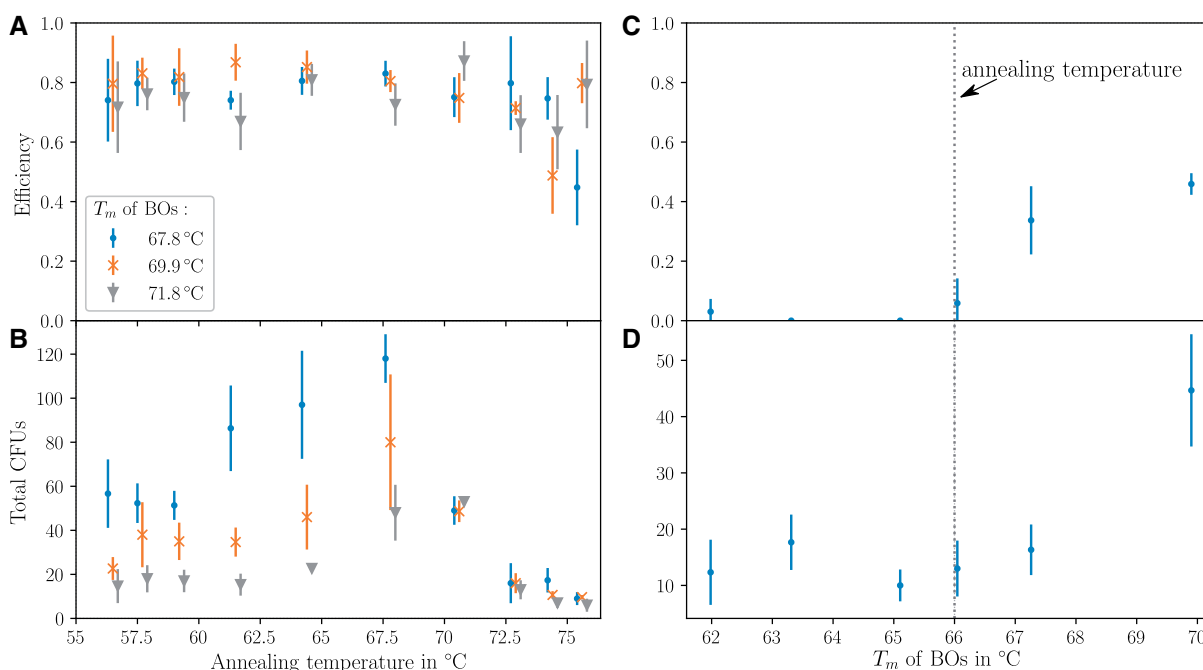
Fig. 3 Adjustment of the annealing temperature and melting temperature of bridging oligo halves of DMSO/betaine-free LCR. The LCRs were performed as triplicates using the same DNA parts and chemically competent cells. The standard deviation for each LCR is indicated by error bars. (**A**) For a better visibility, the bars of the results were shifted with an offset of the annealing temperatures shown on the x-axis. Optimization of the annealing temperature of the seven-part plasmid *via* gradient-LCR. The temperature range for the annealing was 56.5°C to 75.6°C. Three BO-sets with different melting temperatures were used (67.8°C, 69.9°C and 71.8°C). For the three BO-sets the LCR efficiency was at a similar level. It started decreasing at an annealing temperature of more than 70.6°C. (**B**) As already observed, the total amount of colonies increased with a lower BO-T_m. Overall, the LCRs using these BO-sets resulted in a maximum of colonies in a range of ~66–71°C with 2× more colonies (also shown in Supplementary Figure S15). The BO-set sequences of the three sets are shown in Supplementary Table S4. (**C** and **D**) Based on the optimization shown in A and B, the annealing temperature of 66°C was used to investigate the influence of BO-halves with lower T_ms of 62.0°C to 67.3°C. As a reference, the BO-set '71.8°C' from A and B was used. Further decrease of the BO-T_m did not improve the LCR at the optimized annealing temperature of 66°C. In comparison to A and D, the LCR with the BO-set '69.9°C' was less efficient due to loss of function by additional repeated freeze-thaw cycles of the DNA parts and BOs. The sequences of the BO-sets '62.0°C' to '67.3°C' are shown in Supplementary Table S5. BO, bridging oligo; CFU, colony forming unit; DMSO, dimethyl sulfoxide; T_m, melting temperature of a BO-half.

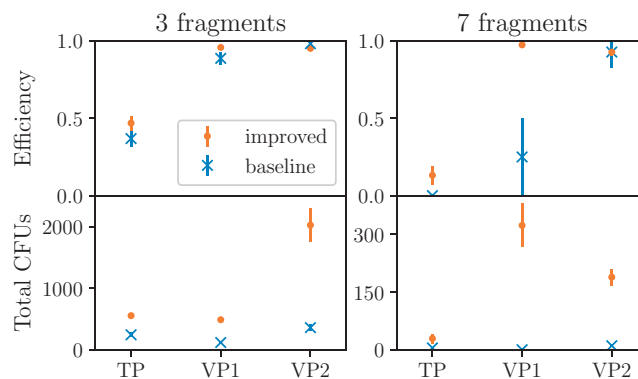**Fig. 4** Comparison of the baseline and the improved LCR protocol for assembling the toy-model plasmid ('TP') and the validation plasmids 1 ('VP1') and 2 ('VP2'). The improved protocol increased the total amount of (correct) colonies for all assemblies. The efficiencies were also improved, although the LCRs of the three-part splits were similar for both protocols. LCRs were performed as triplicates and were transformed by chemical transformation. For the seven-part split LCRs of the toy-model plasmid 'TP' and validation plasmid 'VP1' the LCRs were transformed by electroporation due to low or no colonies when chemical transformation was used. CFU, colony forming unit.

Validation of the improved protocol

To further verify the improved LCR protocol, we designed two validation plasmids based on the reporter genes *lacZ* and one or two antibiotic resistance genes (Supplementary Figures S18 and S19). For both plasmids, a three-part and seven-part split were designed and three protocols were applied: the baseline, improved and a third protocol using BO-sets with a higher target

melting temperature of 74.8°C. According to the results shown in Supplementary Figures S6C and S11A, BOs with a higher T_m may improve the efficiency.

As shown by the optimizations for the toy-model plasmid, the improved LCR protocol is beneficial for the assembly of both splits of the validation plasmids 'VP1' and 'VP2' (Figure 4 and Table 1). Due to high efficiencies when the baseline protocol was applied, the effect of an increased efficiency by the

improved protocol was only seen for the seven-part split of the toy-model plasmid 'TP' and validation plasmid 'VP1'. Nevertheless, the optimized protocol without DMSO/betaine increased the total amount of CFUs in comparison to the baseline protocol. According to the results of the third protocol, higher BO-melting temperatures improved the LCR with DMSO and betaine but with a low impact (Supplementary Figures S21 and S22). In addition, longer BOs are used in this protocol which are typically more expensive. For automated assemblies, the usage of DMSO and betaine would also be disadvantageous.

For both seven-part splits, Sanger sequencing of ten plasmids from CFUs with the correct phenotypes 'blue' and resistance to the antibiotic(s) was performed for each validation plasmid. No false-positives were revealed. Control reactions without BOs and Ampligase® were performed for all splits and revealed no colonies. Additionally, four plasmids from colonies with the wrong phenotype 'white' were analyzed for each validation plasmid. For the validation plasmid 1, the sequences had point-mutations in the 80 bp part of the *lacZ*. This part was ordered as oligonucleotides. This suggests that the mutations are due to the oligonucleotide synthesis. For the validation plasmid 2, three out of four plasmids had a point-mutation in the same *lacZ* part mentioned for the validation plasmid 1. One plasmid lacked the *lacZ*-parts 1 and 2 (parts 4 and 5 of the seven-part split shown in Supplementary Figure S18). Nevertheless, the validation experiments support the improved LCR protocol because the false-negative rate only affects the efficiencies and not the total amount of CFUs.

Besides general factors like the genetic context, total plasmid size, amount of parts, purification grade and freeze-thaw-cycles, the successful optimization of the LCR depends on BOs with melting temperatures which fit the kinetic conditions in the reaction. According to this study, the assembly of two splits of three plasmids showed a negative impact when DMSO and betaine are supplied (Figures 2 and 4) although it is considered to be beneficial in the literature (9).

Conclusion

To our knowledge, the presented assembly of a plasmid with *sfGFP* and *mRFP1* is the first documented experimental LCR-design that includes a direct and fast readout to investigate the influence of various plasmid designs and experimental conditions. The utilized toy-model plasmid in combination with the fluorescence-based analysis enables a robust and easy-to-adapt *in vivo* system to get valuable insights into the LCR and is also adaptable for investigations of other assembly techniques.

Based on this workflow, the impact of intramolecular and intermolecular crosstalk between BOs is assumed to be negligible for the assembly of a seven-part toy-plasmid, whereas a strong interdependence in regards to the addition of DMSO/betaine, the BO-T_m, the annealing temperature and ligation temperature was observed. Those findings were validated by assembling two validation plasmids by comparing the baseline conditions with an improved LCR protocol without DMSO/betaine, a target T_m of 67.8°C for each BO-half and an annealing temperature of 66°C. Related to this, it is of crucial importance to be consistent in the choice of the algorithms for the T_m calculation. Sets with a melting temperature of 67.8°C when using the formula of SantaLucia (20) are recommended. A melting temperature of 65.2°C is recommended when using the algorithms of SantaLucia (20) and the salt correction of Owcarzy et al. (35). Using guanine or cytosine at the 3′-end of the BOs was not found to be beneficial.

In total, we used a new toy-model plasmid to investigate an improved LCR protocol without DMSO/betaine and successfully applied it for the assembly of two validation plasmids. We conclude that our improved LCR protocol will help to achieve more efficient assemblies and to enable a simpler way for automated LCR assemblies by omitting DMSO/betaine and adjustments of the thermal conditions. To ensure reproducible conditions, we provide a step-by-step LCR protocol. You can download it from the digital supplement. We also offer a beta-version of a Geneious-plugin to design LCR-constructs and BOs with the improved parameters at www.gitlab.com/kabischlab.de/lcr-publication-synthetic-biology. In the future, we will provide a web-application and a stand-alone tool for the automated design of LCR-constructs and BOs. To accelerate the screening process, flow cytometry could be applied to use this validated method for future applications to e.g., investigate more rules for the LCR or other assembly methods. Another interesting approach would include the combination of *in vitro* studies using cell-free systems (40) and the toy-model plasmid.

Supplementary data

Supplementary Data are available at SYNBIO Online, including [reference citation(s)].

References

1. Gibson,D.G., Young,L., Chuang,R.-Y., Venter,J.C., Hutchison,C.A. and Smith,H.O. (2009) Enzymatic assembly of DNA molecules up to several hundred kilobases. *Nat. Methods*, 6, 343–345.
2. Engler,C., Kandzia,R. and Marillonnet,S. (2008) A one pot, one step, precision cloning method with high throughput capability. *PLoS One*, 3, e3647.
3. ——, Gruetzner,R., Kandzia,R. and Marillonnet,S. (2009) Golden gate shuffling: a one-pot DNA shuffling method based on type IIs restriction enzymes. *PLoS One*, 4, e5553.
4. Quan,J. and Tian,J. (2009) Circular polymerase extension cloning of complex gene libraries and pathways. *PLoS One*, 4, e6441.
5. Storch,M., Casini,A., Mackrow,B., Fleming,T., Trewhitt,H., Ellis,T. and Baldwin,G.S. (2015) BASIC: a new biopart assembly standard for idempotent cloning provides accurate, single-tier DNA assembly for synthetic biology. *ACS Synth. Biol.*, 4, 781–787.

6. Ma,H., Kunes,S., Schatz,P.J. and Botstein,D. (1987) Plasmid construction by homologous recombination in yeast. *Gene*, 58, 201–216.

7. Torella,J.P., Lienert,F., Boehm,C.R., Chen,J.-H., Way,J.C. and Silver,P.A. (2014) Unique nucleotide sequence-guided assembly of repetitive DNA parts for synthetic biology applications. *Nat. Protoc.*, 9, 2075–2089.

8. Pachuk,C.J., Samuel,M., Zurawski,J.A., Snyder,L., Phillips,P. and Satishchandran,C. (2000) Chain reaction cloning: a one-step method for directional ligation of multiple DNA fragments. *Gene*, 243, 19–25.

9. de Kok,S., Stanton,L.H., Slaby,T., Durot,M., Holmes,V.F., Patel,K.G., Platt,D., Shapland,E.B., Serber,Z., Dean,J. et al. (2014) Rapid and reliable DNA assembly *via* ligase cycling reaction. *ACS Synth. Biol.*, 3, 97–106.

10. Chandran,S. (2017) Rapid assembly of DNA via ligase cycling reaction (LCR). In: R.A.,Hughes (ed). *Synthetic DNA*, Vol. 1472. Springer, New York, NY, pp. 105–110.

11. Roth,T.L., Milenkovic,L. and Scott,M.P. (2014) A rapid and simple method for DNA engineering using cycled ligation assembly. *PLoS One*, 9, e107329.

12. SantaLucia,J. (2007) Physical principles and visual-OMP software for optimal PCR design. In: J.M.,Walker and A.,Yuryev (eds). *PCR Primer Design*, Vol. 402. Humana Press, Totowa, NJ, pp. 3–33.

13. Hendling,M., Pabinger,S., Peters,K., Wolff,N., Conzemius,R. and Barišić,I. (2018) Oli2go: an automated multiplex oligonucleotide design tool. *Nucleic Acids Res.*, 46, W252–W256.

14. Nowak,R.M., Wojtowicz-Krawiec,A. and Plucienniczak,A. (2015) DNASynth: a computer program for assembly of artificial gene parts in decreasing temperature. *BioMed Res. Int.*, 2015, 1–8.

15. Bode,M., Khor,S., Ye,H., Li,M.-H. and Ying,J.Y. (2009) TmPrime: fast, flexible oligonucleotide design software for gene synthesis. *Nucleic Acids Res.*, 37, W214–W221.

16. Robinson,C.J., Dunstan,M.S., Swainston,N., Titchmarsh,J., Takano,E., Scrutton,N.S. and Jervis,A.J. (2018) Chapter thirteen—Multifragment DNA assembly of biochemical pathways via automated ligase cycling reaction. In: N., Scrutton, (ed). *Methods in Enzymology*, Vol. 608 of Enzymes in Synthetic Biology. Academic Press, pp. 369–392. https://www.sciencedirect.com/science/article/pii/S0076687918301459?via%3Dihub.

17. Lee,M.E., DeLoache,W.C., Cervantes,B. and Dueber,J.E. (2015) A highly characterized yeast toolkit for modular, multipart assembly. *ACS Synth. Biol.*, 4, 975–986.

18. Kearse,M., Moir,R., Wilson,A., Stones-Havas,S., Cheung,M., Sturrock,S., Buxton,S., Cooper,A., Markowitz,S., Duran,C. et al. (2012) Geneious basic: an integrated and extendable desktop software platform for the organization and analysis of sequence data. *Bioinformatics*, 28, 1647–1649.

19. Untergasser,A., Cutcutache,I., Koressaar,T., Ye,J., Faircloth,B.C., Remm,M. and Rozen,S.G. (2012) Primer3-new capabilities and interfaces. *Nucleic Acids Res.*, 40, e115.

20. SantaLucia,J. (1998) A unified view of polymer, dumbbell, and oligonucleotide DNA nearest-neighbor thermodynamics. *Proc. Natl. Acad. Sci. USA*, 95, 1460–1465.

21. Bernhart,S.H., Tafer,H., Flamm,C., Stadler,P.F. and Hofacker,I.L. (2006) Partition function and base pairing probabilities of RNA heterodimers. *Algorithms Mol. Biol.*, 2006, 1.

22. McCaskill,J.S. (1990) The equilibrium partition function and base pair binding probabilities for RNA secondary structure. *Biopolymers*, 29, 1105–1119.

23. Zuker,M. and Stiegler,P. (1981) Optimal computer folding of large RNA sequences using thermodynamics and auxiliary information. *Nucleic Acids Res.*, 9, 133–148.

24. Dimitrov,R.A. and Zuker,M. (2004) Prediction of hybridization and melting for double-stranded nucleic acids. *Biophys. J.*, 87, 215–226.

25. Lorenz,R., Bernhart,S.H., Höner zu Siederdissen,C., Tafer,H., Flamm,C., Stadler,P.F. and Hofacker,I.L. (2011) ViennaRNA Package 2.0. *Algorithms Mol. Biol.*, 6, 26.

26. Kirkpatrick,S., Gelatt,C.D. and Vecchi,M.P. (1983) Optimization by simulated annealing. *Science*, 220, 671–680.

27. Galassi,M., Davies,J., Theiler,J., Gough,B., Jungman,G., Booth,M. and Rossi,F. (2009) *GNU Scientific Library Reference Manual*, 3rd edn. ISBN: 0954612078.

28. Zhang,Y., Werling,U. and Edelmann,W. (2012) SLiCE: a novel bacterial cell extract-based DNA cloning method. *Nucleic Acids Res.*, 40, e55.

29. Jacobus,A.P. and Gross,J. (2015) Optimal cloning of PCR fragments by homologous recombination in *Escherichia coli*. *PLoS One*, 10, e0119221.

30. von Ahsen,N., Wittwer,C.T. and Schütz,E. (2001) Oligonucleotide melting temperatures under PCR conditions: nearest-neighbor corrections for Mg^{2+}, deoxynucleotide triphosphate, and dimethyl sulfoxide concentrations with comparison to alternative empirical formulas. *Clin. Chem.*, 47, 1956–1961.

31. Dutra,B.E., Sutera,V.A. and Lovett,S.T. (2007) RecA-independent recombination is efficient but limited by exonucleases. *Proc. Natl. Acad. Sci. USA*, 104, 216–221.

32. Bzymek,M. and Lovett,S.T. (2001) Instability of repetitive DNA sequences: the role of replication in multiple mechanisms. *Proc. Natl. Acad. Sci. USA*, 98, 8319–8325.

33. Geissmann,Q. (2013) OpenCFU, a new free and open-source software to count cell colonies and other circular objects. *PLoS One*, 8, e54072.

34. Carpenter,A.E., Jones,T.R., Lamprecht,M.R., Clarke,C., Kang,I.H., Friman,O., Guertin,D.A., Chang,J.H., Lindquist,R.A., Moffat,J. et al. (2006) CellProfiler: image analysis software for identifying and quantifying cell phenotypes. *Genome Biol.*, 7, R100.

35. Owczarzy,R., Moreira,B.G., You,Y., Behlke,M.A. and Walder,J.A. (2008) Predicting stability of DNA duplexes in solutions containing magnesium and monovalent cations. *Biochemistry*, 47, 5336–5353.

36. Escara,J.F. and Hutton,J.R. (1980) Thermal stability and renaturation of DNA in dimethyl sulfoxide solutions: acceleration of the renaturation rate. *Biopolymers*, 19, 1315–1327.

37. Henke,W., Herdel,K., Jung,K., Schnorr,D. and Loening,S.A. (1997) Betaine improves the PCR amplification of GC-rich DNA sequences. *Nucleic Acids Res.*, 25, 3957–3958.

38. Hanahan,D. (1983) Studies on transformation of *Escherichia coli* with plasmids. *J. Mol. Biol.*, 166, 557–580.

39. Davis,D.L., O'Brie,E.P. and Bentzley,C.M. (2000) Analysis of the degradation of oligonucleotide strands during the freezing/thawing processes using MALDI-MS. *Anal. Chem.*, 72, 5092–5096.

40. Shin,J. and Noireaux,V. (2012) An *E. coli* cell-free expression toolbox: application to synthetic gene circuits and artificial cells. *ACS Synth. Biol.*, 1, 29–41.